The Astrophysical Journal, 711:1057–1061, 2010 March 10 doi:10.1088/0004-637X/711/2/1057

A FLUX ROPE ERUPTION TRIGGERED BY JETS

Juan Guo[1], Yu Liu[2], Hongqi Zhang[1], Yuanyong Deng[1], Jiaben Lin[1], and Jiangtao Su[1]
[1] Key Laboratory of Solar Activity, National Astronomical Observatories, Beijing 100012, China; guojuan@bao.ac.cn
[2] Yunnan Astronomical Observatory, National Astronomical Observatories, Kunming 650011, China
Received 2009 November 22; accepted 2010 January 25; published 2010 February 22

ABSTRACT

We present an observation of a filament eruption caused by recurrent chromospheric plasma injections (surges/jets) on 2006 July 6. The filament eruption was associated with an M2.5 two-ribbon flare and a coronal mass ejection (CME). There was a light bridge in the umbra of the main sunspot of NOAA 10898; one end of the filament was terminated at the region close to the light bridge, and recurrent surges were observed to be ejected from the light bridge. The surges occurred intermittently for about 8 hr before the filament eruption, and finally a clear jet was found at the light bridge to trigger the filament eruption. We analyzed the evolutions of the relative darkness of the filament and the loaded mass by the continuous surges quantitatively. It was found that as the occurrence of the surges, the relative darkness of the filament body continued growing for about 3–4 hr, reached its maximum, and kept stable for more than 2 hr until it erupted. If suppose 50% of the ejected mass by the surges could be trapped by the filament channel, then the total loaded mass into the filament channelwill be about 0.57×10^{16} g with a momentum of 0.57×10^{22} g cm s^{-1} by 08:08 UT, which is a non-negligible effect on the stability of the filament. Based on the observations, we present a model showing the important role that recurrent chromospheric mass injection play in the evolution and eruption of a flux rope. Our study confirms that the surge activities can efficiently supply the necessary material for some filament formation. Furthermore, our study indicates that the continuous mass with momentum loaded by the surge activities to the filament channel could make the filament unstable and cause it to erupt.

Key words: Sun: activity – Sun: coronal mass ejections (CMEs) – Sun: filaments, prominences

1. INTRODUCTION

The Hα surges were straight or slightly curved mass ejections stretching out and away from small flare-like brightenings at footpoints in the chromosphere into coronal heights. They usually moved upward at 20–200 km s^{-1}, reached heights of up to 200,000 km, and typically lasted for 10–20 minutes (Roy 1973a; Bruzek & Durrant 1977). They can be seen as dark features on the solar disk and usually showed a strong trend toward recurrence. Surge activities were often associated with certain types of magnetic activity around their bases in the photosphere, such as satellite polarity (Gopasyuk & Ogir 1963; Rust 1968; Roy 1973a), evolving magnetic features (Roy 1973a), moving magnetic bipolers (Canfield et al. 1996), and light bridge in the umbra of sunspot (Roy 1973b; Asai et al. 2001). Shibata et al. (1992) and Yokoyama & Shibata (1995, 1996) show in their two-dimensional MHD numerical simulations that magnetic reconnection between emerging magnetic fluxes and pre-existing fields actually produce adjacent hot (X-ray) and cold (Hα) plasma ejections simultaneously. The relationship between chromosphere surges and similar ejection phenomena at other wavelengths, such as UV, EUV, and X-ray jets, have also been studied by a number of authors (Schmahl 1981; Schmieder et al. 1984, 1993; Svestka et al. 1990; Shibata et al. 1992; Chae et al. 1999; Canfield et al. 1996; Shimojo et al. 1996; Zhang et al. 2000; Asai et al. 2001; Liu & Kurokawa 2004; Jiang et al. 2007a, 2007b; Chen et al. 2008).

A few studies have shown that there is a close correlation between filament formation and surge activity. For the first time, Zirin (1976) studied the relationship between surge activity and filament formation. He reported a short-lived filament produced by a surge ejection, that is, part of a large surge material was trapped in the solar atmosphere, forming an obvious dark filament. The filament lasted for about 30 minutes, then rose up and returned to the source of the surge. Unfortunately, little attention was paid to this special phenomenon and the associated physical process, mainly due to the quick disappearance of this filament and the fact that there have been no convincing samples reported since then. Recently, Liu et al. (2005a) also found that some filaments can be quickly formed in the corona by trapping the cold material supplied by surges originating from the chromosphere. They also found a newly formed filament that existed on the solar surface for not less than 20 hr without erupting.

Still a few studies show that there is a relationship between large-scale CMEs and small-scale surges/jets, in contrast to energetic flares and eruptive filaments. In a statistical study of 25 CME events with definite associations, Munro et al. (1979) pointed out that there were five CMEs without an accompanying eruptive filament but with Hα surges or sprays. Liu et al. (2005b) reported a close temporal and spatial relationship between a well-observed emerging flux region (EFR) surge and its associated jet-like CMEs. However, no filament was involved in the surge–CME event in this study. Liu (2008) studied 10 large surges and classified them into three types: jet-like, diffuse, and close loop. He found that the jet-like surges were always associated with jet-like CMEs; the diffuse surges were associated with wide-angle CMEs; and the closed-loop surges were not associated with CMEs. Wang et al. (2001) showed that an interactive loop can be activated by a surge to trigger flare and CME. In their study, the surge quickly turned into a set of disturbances and they suggested that such disturbance may represent mass transfer and cause the transport of field lines. Recently, Jiang et al. (2008) reported a rare observation of direct magnetic interaction between a trans-equatorial jet and interconnecting loops in the southern hemisphere. Thereafter, two CMEs were observed within 2 hr in association with the event.

On 2006 July, a filament eruption in NOAA 10898 (S08W42) was observed by some ground-based and space telescopes. The eruption was accompanied by a flare of X-ray class M2.5 and an

SW-directed halo type CME. We noticed that before the eruption of the filament there were recurrent surges near one footpoint of the filament. We also found a close correlation between the occurrence of the surges and the evolution and eruption of the filament.

2. OBSERVATION AND DATA REDUCTION

We used data from various ground-based and space solar telescopes. They include the following.

1. More than 10 hr of Hα filtergrams obtained by the Hα telescope on the the Solar Magnetism and Activity Telescope (SMAT; Zhang et al. 2007; Su & Zhang 2007) at the Huairou Solar Observing Station (HSOS). The SMAT is comprised of two telescopes. One is for the measurement of full-disk video vector magnetic field observations at 5324.19 Å. Another is for the full-disk Hα images at Hα line center. The CCD of the Hα telescope is 2K×2K with $1''$ pixel^{-1}.
2. Line-of-sight magnetograms were observed by the Michelson Doppler Imager (MDI) on board the *Solar and Heliospheric Observatory* (*SOHO*). For the data used in the current study, the cadence is 90 minutes and the spatial resolution is about $2''$ pixel (Scherrer et al. 1995).
3. White-light (5000 Å, broad band) and EUV ($Fe_{IX/X}$ 171 Å) observations were obtained by the *Transition Region and Corona Explorer* (*TRACE*; Handy et al. 1999; Schrijver et al. 1999). The pixel size is about $0''.5$.

For all full-disk images, the alignments are very easy. We find the center and radius of each image by limb fitting and make rotational adjustment by visual inspection. For the co-alignment of *TRACE* and other images, we use *TRACE* white-light images and MDI white-light images at the same time by fitting the sunspots.

3. RESULTS

Figure 1 contains a sequence of images of this event: a *TRACE* white-light image (Figure 1(a)), a *TRACE* 171 Å image (Figure 1(b)), an MDI magnetogram (Figure 1(c)), and an Hα center image (Figure 1(d)). The black curve in Figure 1(a) is the jet profile according to the jet in Figure 1(b). The white curve in Figure 1(c) is the filament profile according to the filament in Figure 1(d). A light bridge was found in the umbra of the main sunspot in the active region NOAA 10898. The jet was ejected from the light bridge, and one end of the filament was found to be terminated at the region close to the light bridge.

From the Hα images, the surges that were observed to be ejected from the light bridge occurred intermittently at least 8 hr before the filament eruption. After the filament eruption an EFR with opposite polarity appeared at the top terminal of the light bridge. The occurrences of the surges were marked by two rows of thick lines at the top of Figure 4. There were many small surges ejected from the light bridge (indicated by the second row of thick lines in Figure 4). In addition, there were still two relatively large surges ejected from the north corner of the light bridge (indicated by the first row of thick lines in Figure 4).

Figure 2 demonstrates the time sequence of Hα center and *TRACE* 171 Å images showing the main evolution and eruption of the filament. From upper panels of the Hα images, it was found that the filament body continued growing during the previous 3–4 hr. The filament began to bifurcate from 07:30 UT. At 08:04 UT, the filament was apparently composed of several threads that seemed linked together. During 8:11–08:12 UT, a bright jet appeared at the north corner of the light bridge (indicated by an arrow at 08:12 UT). During 08:15–8:20 UT, a surge (indicated by an arrow at 08:18 UT) was ejected from the light bridge into the filament channel; meanwhile, the bottom-left part of the filament weakened and disappeared in the Hα images and two initial brightening points appeared. Then, the filament erupted gradually and the flare appeared. From the bottom panel of the *TRACE* 171 Å images, it was found that a bright jet appeared at the N corner of the light bridge at 08:10 UT (indicated by an arrow at 08:10 UT); in the following 8 minutes, a good sequence of material was ejected from the same place into the filament channel. As a consequence, the filament became very active, then lost its equilibrium and erupted. It should be mentioned that although the initial brightening points in Hα images took place beneath the filament, the initial disturbance of the filament came from the surges near one of its footpoints, which was very clear in the high resolution *TRACE*171 Å images.

The evolution of the relative darkness of the filament would provide an important clue regarding the evolution of the filament mass. We calculated the relative darkness of the filament as follows: first, we choose four quiet regions, which were located at the top, bottom, left, and right sides of the filament, respectively, to get the mean darkness of the quiet region($D_{\rm quiet}$) by averaging the darkness of the four regions; second, we chose a region (corresponding to the box at 06:22 UT in Figure 2) covering the main region of the filament to calculate the relative darkness of the filament; we then defined a threshold ($D_{\rm threshold} = D_{\rm quiet} - 16$) and the pixel in the region with a darkness darker than the threshold was regarded as the filament mass (D_i is the darkness of such pixel); finally, the relative darkness of the filament could be calculated by the equation $\sum (D_i - D_{\rm threshold}/D_{\rm threshold})$. As an example, we presented a set of images that was compiled for the calculation of the relative darkness of the filament at 06:22 UT (Figure 3). The initial image from which we chose to calculate the relative darkness of the filament is shown in Figure 3(a). By averaging the darkness of the four quiet regions from the Hα image at 06:22 UT in Figure 2, we obtained the mean value of the darkness of the quiet region $D_{\rm quiet}$ as 411.0685 and the threshold $D_{\rm threshold}$ as 395.069 for the image in Figure 3(a). Thus, the pixels whose values are less than 395.069 were treated as the filament mass. Thereafter, some pixels with a value less than 395.069, excluding the filament mass were excluded first as shown in Figure 3(c). The pixels in the region of the sunspot were replaced with $D_{\rm quiet}$ (in Figure 3(b)) for the same reason. The filament area that was determined are the white regions in Figure 3(d). According to the above equation, the relative darkness of the filament at 06:22 UT was 124.874. Using the Hα center filtergrams obtained by SMAT/HSOS, we calculated the relative darkness of the filament and show the result in Figure 4 by two solid curves and some diamonds. For the curve from 00:45 to 04:00 UT, the relative darkness of the filament continued growing for about 3–4 hr as the occurrence of the intermittent surges and the slope of the linearly fitted line is 0.94. From 04:00 to 05:43 UT, the calculated relative darkness of some images were shown as individual diamonds and the analysis of the evolution of the relative darkness was omitted, because the Hα observation stopped for about 1 hr (from 04:10 to 05:10 UT) due to bad seeing and the images before 04:10 and after 05:10 were also not quite good. For the curve from 05:43 to 08:30 UT, the relative darkness of the filament reached its maximum and stayed relatively stable for more than 2 hr until its eruption.

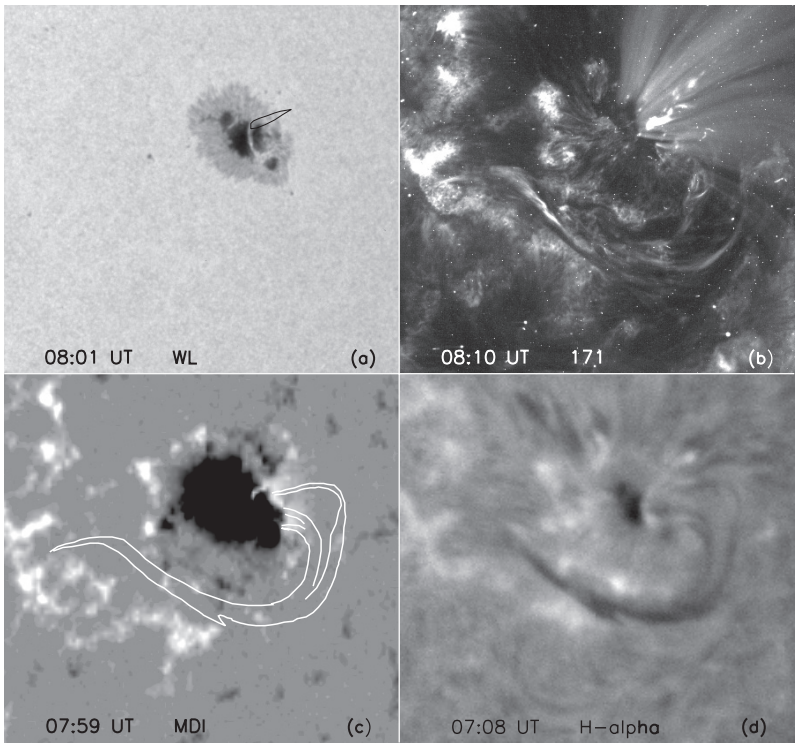

Figure 1. Sequence of images of this event. (a) *TRACE* white-light image of NOAA 10898. (b) *TRACE* 171 Å image. (c) MDI magnetogram. (d) Hα center image. The black curve in (a) corresponds to the jet in (b). The white curve in (c) corresponds to the filament profile in (d). The field of view of each frame is about 225″ × 210″.

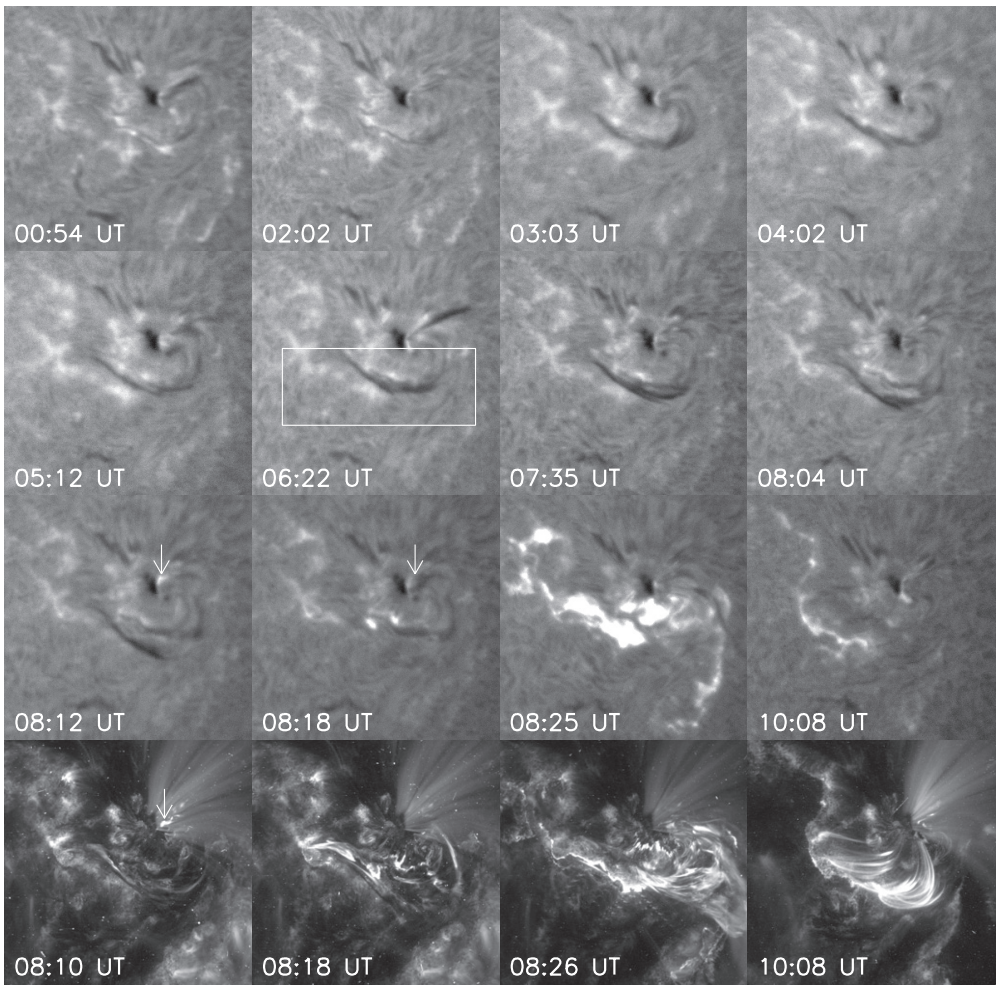

Figure 2. Time sequence of Hα and *TRACE* 171 Å images showing the evolution and eruption of the filament. The field of view is about 300″ × 296″.

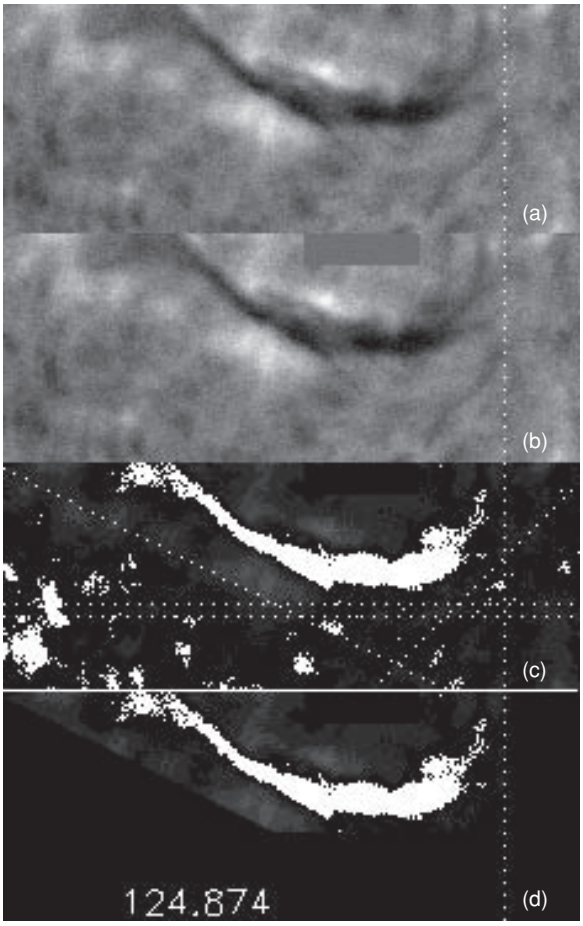

Figure 3. Sequence of images showing how we get the area of the filament to calculate the relative darkness of the filament.

The corresponding linearly fitted line showed a slight trend of decrease with a slope −0.37.

To further examine the relationship between the intermittent surges and the filament, we also estimated the amount of the mass ejected by the surge and show the result in Figure 4 as a dashed curve with cycles. We used some observed values: velocity $v = 10^6$ cm s^{-1}, area at the base of the surge $A = 10^{17}$ cm^2, the durations of surges Δt, and typical chromospheric density $\rho \approx 10^{-11}$ g cm^{-3}. The amount of mass ejected by the surges was $\sum \rho A v \Delta t$. If suppose 50% of the ejected mass could be trapped by the filament channel, the amount of loaded mass by the surges to the filament channel will be $0.5 \times \sum \rho A v \Delta t$. From Figure 4, it was found that the profiles and trends of the amount of loaded mass by surges and of relative darkness of the filament were consistent during 00:45–04:00 UT. Usually, the typical filament mass was about 10^{16} g. For this event, by 06:30 UT about 0.5×10^{16} g mass with a momentum of 0.5×10^{22} g cm s^{-1} has been loaded into the filament channel, which is a non-negligible effect on the stablility of the filament. Then as the mass was injected by the following surges, the filament began to bifurcate after 07:35 UT and finally erupted at 08:12 UT. By 08:08 UT, the total loaded mass into the filament channel was about 0.57×10^{16} g with a momentum of 0.57×10^{22} g cm s^{-1}.

4. CONCLUSION AND DISCUSSION

We have presented a complementary observation of a surge–filament triggering a flare–CME process on 2006 July 6. This

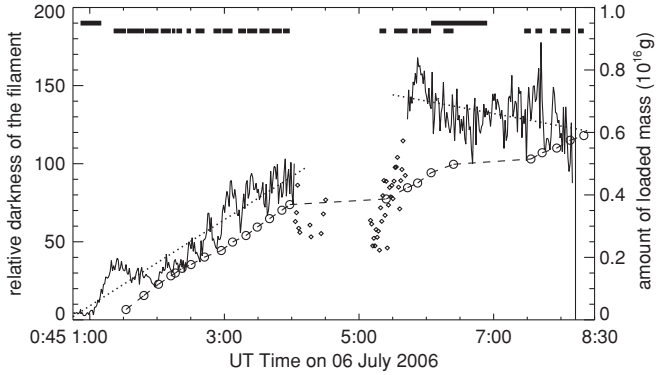

Figure 4. Two rows of thick lines at the top of this figure indicate the recurrent surges. The two solid curves are the relative darkness of the filament during 00:45–04:00 UT and 05:43–08:30 UT. The two dotted lines are the linearly fitted lines for the two parts, with slopes of 0.94 and −0.37, respectively. The individual diamonds are some poor data because of bad seeing during 04:00–05:43 UT. The dashed curve with cycles is the amount of mass loaded by the intermittent surges. The vertical solid line is the beginning of the flare.

event manifests itself as recurrent surges and filament eruption resulting in an M2.5 two-ribbon flare and a SW-directed CME with a speed of 600 km s^{-1}. More than 10 hr of Hα center observations showed that the surges ejected intermittently from the light bridge in the umbra of the sunspot NOAA 10898 for at least 8 hr before the eruption of the filament. We quantitatively analyzed the evolutions of the relative darkness of the filament and the loaded mass by the continuous surges. It was found that as the occurrence of the intermittent surges, the relative darkness of the filament body continued growing for about 3–4 hr, reached its maximum, and was stable for more than 2 hr until it erupted. If suppose 50% of the mass ejected by the surges could be trapped by the filament channel, then the total loaded mass into the filament channel will be about 0.57×10^{16} g with a momentum of 0.57×10^{22} g cm s^{-1} by 08:08 UT, which is a non-negligible effect on the stablility of the filament. From the 171 Å images, it was found that the filament eruption was triggered by a clear jet at 08:10 UT.

Usually, the surges are mass ejected along straight or slightly curved open magnetic field lines, while the filament is situated in a cavity. Why would the surges inject material to the filament channel? Liu et al. (2005a) have pointed out that the open coronal lines along which a surge ejected can exist in the filament channel as axial fields. Following them and based on the above observation characteristics, we present a sequence of models to show the important role of recurrent chromospheric mass injection in the evolution and eruption of a filament. Figures 5(a) and (b) show that when a newly emerging feature appeared near a filament channel, the reconnection could occur between the newly emerging magnetic feature and the nearby coronal line which is located in the filament channel as axial fields. Under this condition, the mass ejection by surges can been trapped by the nearby filament channel. Figure 5(c) shows a surge injection and the consequent eruption of the filament.

The above morphological and quantitative analyses indicate that there is a close relationship between the filament development and the chromospheric ejections. The many recurrent surges before the filament eruption must input more and more mass into the filament channel, which should result in the mass increase of the filament and then bifurcation of the filament. Our study confirms that the surge activities can efficiently supply the necessary material for some filament formation (Liu et al. 2005a). Furthermore, in this study, the continuous

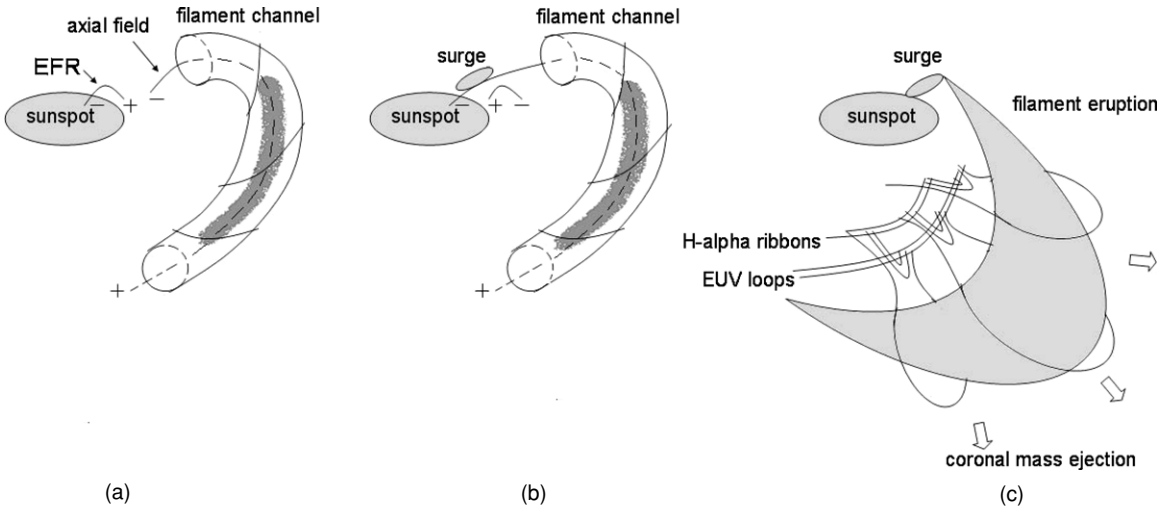

Figure 5. Sequence of models showing the relationship between the surges and the filament: (a) the emerging flux rope (EFR) appeared near the axial field of the filament channel. (b) Reconnection occurred between EFR and the axial field line. Then the surge could be trapped along the axial field into the filament channel. (c) Surge injection and the consequent filament eruption.

mass with momentum loaded by the surge activities to the filament channel could make the filament unstable and erupt. The jet played a trigger for the filament to lose its original equilibrium and erupt at the end.

In order to further confirm the association between the recurrent surges and the evolution and eruption of the filament, we have investigated the temporal evolution of Hα center observation from Kanzelhohe Solar Observatory (KSO) in Austria and found the same result.

We thank the referee for the comments that helped us to improve the paper. We thank HSOS Observatory, Kanzelhoehe Observatory, *SOHO* and *TRACE* teams for the high-quality data supplied.

This study is supported by the National Natural Science Foundation of China (10733020, 10911120051, 0911181001, 10933003), the National Basic Research Program of China (2006CB806301), and the Young Researcher Grant of the National Astronomical Observatories, Chinese Academy of Sciences.

REFERENCES

Asai, A., Ishii, T., & Kurokawa, H. 2001, ApJ, 555, L65
Bruzek, A., & Durrant, C. J. 1977, Astrophysics and Space Science Library, Vol. 69, Illustrated Glossary for Solar and Solar-Terrestrial Physics (Dordrecht: Reidel)
Canfield, R. C., Reardon, K. P., Leka, K. D., Shibata, K., Yokoyama, T., & Shimojo, M. 1996, ApJ, 464, 1016
Chae, J., Qiu, J., Wang, H., & Goode, P. 1999, ApJ, 464, 1016
Chen, H. D., Jiang, Y. C., & Ma, S. L. 2008, A&A, 478, 907
Handy, B. N., et al. 1999, Sol. Phys., 187, 229
Gopasyuk, S. I., & Ogir, M. B. 1963, Izv. Krymsk. Astrofiz. Obs., 30, 185
Jiang, Y., Chen, H., Li, K., Shen, Y., & Yang, H. 2007a, A&A, 469, 331
Jiang, Y., Shen, Y., Yi, B., Yang, J., & Wang, J. 2008, ApJ, 677, 699
Jiang, Y., Yang, L., Li, K., & Ren, D. 2007b, ApJ, 662, L131
Liu, Y. 2008, Sol. Phys., 249, 75
Liu, Y., & Kurokawa, H. 2004, ApJ, 610, 1136
Liu, Y., Kurokawa, H., & Shibata, K. 2005a, ApJ, 631, L93
Liu, Y., Su, J. T., Morimoto, T., Kurokawa, H., & Shibata, K. 2005b, ApJ, 628, 1056
Munro, R. H., Gosling, J. T., Hildner, E., MacQueen, R. M., Poland, A. I., & Ross, C. L. 1979, Sol. Phys., 61, 201
Roy, J. R. 1973a, Sol. Phys., 28, 95
Roy, J. R. 1973b, Sol. Phys., 32, 138
Rust, D. M. 1968, in IAU Symp. 35, Structure and Development of Solar Active Regions, ed. K. O. Kiepenheuer (Dordrecht: Kluwer), 77
Scherrer, P. H., et al. 1995, Sol. Phys., 162, 129
Schmahl, E. 1981, Sol. Phys., 162, 169
Schrijver, C. J., et al. 1999, Sol. Phys., 187, 26
Schmieder, B., Mein, P., Martres, M. J., & Tandberg-Hanssen, E. 1984, Sol. Phys., 94, 133
Schmieder, B., van Driel-Gesztelyi, L., Gerlei, O., & Simnett, G. 1993, Sol. Phys., 146, 163
Shibata, K., et al. 1992, PASJ, 44, L173
Shimojo, M., et al. 1996, PASJ, 48, 123
Su, J. T., & Zhang, H. Q. 2007, ApJ, 666, 559
Svestka, Z., Farni, F., & Tang, F. 1990, Sol. Phys., 127, 149
Wang, H. M., Chae, J., Yurchyshyn, V., Yang, G., Steinegger, M., & Goode, P. 2001, ApJ, 559, 1171
Yokoyama, T., & Shibata, K. 1995, Nature, 375, 42
Yokoyama, T., & Shibata, K. 1996, PASJ, 48, 353
Zhang, J., Wang, J., & Liu, Y. 2000, A&A, 361, 759
Zhang, H. Q., et al. 2007, ChJAA, 7, 281
Zirin, H. 1976, Sol. Phys., 50, 399